Spectral changes in layered f-electron systems induced by Kondo hole substitution in the boundary layer

Sudeshna Sen,[1] J. Moreno,[2,3] M. Jarrell,[2,3] and N. S. Vidhyadhiraja[2,4,*]

[1]*Chemistry and Physics of Materials Unit, JNCASR, Bangalore-560064, Karnataka, India*

[2]*Department of Physics & Astronomy, Louisiana State University, Baton Rouge, Louisiana 70803, USA*

[3]*Center for Computation and Technology, Louisiana State University, Baton Rouge, Louisiana 70803, USA*

[4]*Theoretical Sciences Unit, JNCASR, Bangalore-560064, Karnataka, India*

(Received 27 November 2014; revised manuscript received 2 April 2015; published 27 April 2015)

We investigate the effect of disorder on the dynamical spectrum of layered f-electron systems. With random dilution of f sites in a single Kondo insulating layer, we explore the range and extent to which Kondo hole incoherence can penetrate into adjacent layers. We consider three cases of neighboring layers: band insulator, Kondo insulator, and simple metal. The disorder-induced spectral weight transfer, used here for quantification of the proximity effect, decays algebraically with distance from the boundary layer. Further, we show that the spectral weight transfer is highly dependent on the frequency range considered as well as the presence of interactions in the clean adjacent layers. The changes in the low-frequency spectrum are very similar when the adjacent layers are either metallic or Kondo insulating, and hence are independent of interactions. In stark contrast, a distinct picture emerges for the spectral weight transfers across large energy scales. The spectral weight transfer over all energy scales is much higher when the adjacent layers are noninteracting as compared to when they are strongly interacting Kondo insulators. Thus, over all scales, interactions screen the disorder effects significantly. We discuss the possibility of a crossover from non-Fermi-liquid to Fermi-liquid behavior upon increasing the ratio of clean to disordered layers in particle-hole asymmetric systems.

DOI: 10.1103/PhysRevB.91.155146 PACS number(s): 71.27.+a, 79.60.Jv, 71.23.−k

I. INTRODUCTION

Several surprises have emerged through extensive experimental and theoretical investigations of layered correlated systems over the last decade. The pioneering study of Ohtomo *et al.* led to the discovery of a two-dimensional electron gas at the interface of Mott insulating $LaTiO_3$ and band insulating $SrTiO_3$ in atomically resolved heterostructures [1]. A dimensional driven crossover from metal to insulator transition [2] and an anomalous effective mass enhancement [3] was observed by Yoshimatsu *et al.* in digitally controlled $SrVO_3$ thin films. Theoretical predictions in this regard had been reported and semiquantitatively explained by Okamoto *et al.* in Ref. [4]. An early work in this regard may also be found in Ref. [5]. In general, strongly correlated interfaces exhibit several other unexpected properties such as superconductivity [6], coexistence of ferromagnetism and superconductivity [7], and electronic phase separation [8]. Such investigations have led to a renewed focus on a number of intriguing aspects of layered systems. Some of these issues are due to atomic reconstruction, enhanced correlation effects due to reduced coordination number and emergent energy scales owing to the presence of disparate orbital, charge, and spin degrees of freedom [9].

A significant number of theoretical studies on the proximity effects of electron-electron interaction in layered systems have been carried out. Such studies include proximity effects in Hubbard layers [10–18], Falicov-Kimball layers [19], or f-electron superlattices [20,21]. Zenia *et al.* [12] demonstrated that a Mott insulator transforms to a "fragile" Fermi liquid if sandwiched between metallic leads. Helmes *et al.* [17] studied interfaces of strongly correlated metals with Mott insulators. The rate of decay of the quasiparticle weight into the Mott insulator was quantified and further corroborated in the spirit of a Ginzburg-Landau mean-field treatment. Ishida and Liebsch [15] investigated the effect of an interplanar Coulomb interaction using the cellular dynamical mean-field theory (DMFT) and observed a nonlocal correlation induced reduction of the proximity effect. Cluster extensions of DMFT were employed by Okamoto *et al.* in Ref. [22] to examine the proximity effect in superlattices involvng cuprates, predicting a novel enhancement in the superconducting transition temperature.

Recent experimental investigations of heavy fermion (f-electron) superlattices indicate a fascinating interplay of heavy fermion physics, low dimensionality, and interface effects [23]. In the heavy fermion superlattices $m$$CeIn_3$-$n$$LaIn_3$, by reducing the thickness of the $CeIn_3$ layers grown on metallic $LaIn_3$, it was demonstrated that the dimensionality of the f electrons and the magnetic order could be controlled. These dimensionally confined heavy fermion systems then displayed non-Fermi liquid properties that manifested as a linear temperature dependence in resistivity, $\rho_{xx} \sim T$, with a T^2 behavior recovered on increasing the number of $CeIn_3$ layers. This has been followed up with very recent theoretical investigations of the Kondo effect and dimensional crossover in f-electron superlattices [20,21,24]. Tada *et al.* [21] analyzed the formation of heavy electrons in f-electron multilayers. They demonstrated the existence of two (in-plane and out of plane) coherence temperatures in such systems. This implies a crossover in dimensionality of the heavy fermions from two to three dimensions as the temperature and the geometry of the system change. In a study of interfaces of Kondo lattice layers and normal metals, Peters *et al.* [20] showed that such a coupling transformed the full gap of the Kondo lattice layers into a vanishing soft gap. They also demonstrated the strong influence of the Kondo effect on the density of states of the metallic

*raja@jncasr.ac.in

layer. This proximity effect was further shown to be strongly dependent on the number of noninteracting metallic layers.

Although the proximity effects of strong interactions have been addressed quite rigorously, the effects of disorder have not been considered. Incoherent scattering due to impurities is inevitable in heterogeneous interfaces and therefore the physical effects stemming from disorder could be significant. In fact, in heavy fermion compounds, when magnetic sites are substituted by nonmagnetic impurities a substantial reduction of the coherence temperature $T_{\rm coh}$ occurs [25]. Shimozawa *et al.* studied the effects of Kondo hole disorder on epitaxial thin films of divalent-Yb substituted $CeCoIn_5$ [26]. It has been shown by Kaul and Vojta [27] that a randomly depleted Kondo lattice displays nanoscale inhomogeneities exhibiting distinct non-Fermi liquid characteristics. Recently, it has also been shown, in Ref. [28], that dynamical scattering from Kondo holes also yield a non-Fermi liquid behavior for bulk systems. Hence a theoretical study of Kondo hole substituted f-electron interfaces is highly relevant.

In this work, we have explored the spectral dynamics of a single substitutionally disordered Kondo-insulator layer at the boundary of several clean layers of which three types have been considered: (i) noninteracting metals, (ii) band insulators, and (iii) strongly interacting Kondo insulators. We have investigated the penetration of disorder-induced impurity scattering into the proximal layers. An interplay of interactions and Kondo hole disorder lead to significant differences in the spectral weight transfer at low frequencies versus the overall spectrum. We argue that, for non-particle-hole symmetric systems, the systematic addition of clean interacting layers to the substitutionally disordered interface could lead to a gradual crossover from non-Fermi liquid to Fermi liquid behavior. The paper is organized as follows. The model and methods are described in the next section. The results and discussion follow in Sec. III. Our conclusions are presented in the final section.

II. MODEL AND METHOD

The Hamiltonian of a heavy fermion layered system may be constructed through a slight generalization of the standard periodic Anderson model (PAM) as

$$\begin{aligned}\mathcal{H} = &-\sum_{ij\alpha\sigma} t^{||}_{i\alpha j\alpha}(c^{\dagger}_{i\alpha\sigma}c_{j\alpha\sigma}+\text{H.c.}) + \sum_{i\alpha\sigma} V_{\alpha}(f^{\dagger}_{i\alpha\sigma}c_{i\alpha\sigma}+\text{H.c.})\\ &+\sum_{i\alpha\sigma}(\epsilon_{c\alpha}c^{\dagger}_{i\alpha\sigma}c_{i\alpha\sigma}+\epsilon_{f\alpha}f^{\dagger}_{i\alpha\sigma}f_{i\alpha\sigma})\\ &+\sum_{\alpha} U_{\alpha}n_{fi\alpha\uparrow}n_{fi\alpha\downarrow} - \sum_{i\alpha\sigma} t^{\perp}_{\alpha\alpha+1}(c^{\dagger}_{i\alpha\sigma}c_{i\alpha+1\sigma}+\text{H.c.}),\end{aligned} \tag{1}$$

where $t^{||}_{i\alpha j\alpha}$ represents the in-plane hopping between the conduction band (c-electron) orbitals at sites i and j, in the plane α; $\epsilon_{c\alpha}$ and $\epsilon_{f\alpha}$ are the on-site energies of the c and f electrons, respectively; V_{α} is the hybridization between the heavy f and the c electrons in the plane α; U_{α} is the on-site Coulomb repulsion between two electrons occupying an f orbital in the plane α; and $t^{\perp}_{\alpha\alpha+1}$ represents the interplane hopping between the delocalized c orbitals. We explicitly assume here that the f orbitals being local have negligible overlap between the layers.

For an isolated Kondo insulator, the c- and f-electron Greens functions are given by

$$G^{c}(\omega) = \left[\omega^{+} - \frac{V^2}{\omega^{+}-\Sigma_f(\omega)} - \Delta(\omega)\right]^{-1}, \tag{2}$$

$$G^{f}(\omega) = \left[\omega^{+} - \Sigma_f(\omega) - \frac{V^2}{\omega^{+}-\Delta(\omega)}\right]^{-1}. \tag{3}$$

In Eq. (2), we define a purely local, *effective*, conduction electron self-energy, which is related to the f-electron self-energy by, $\Sigma_c(\omega) = \frac{V^2}{\omega^{+}-\Sigma_f(\omega)}$, $\Sigma_f(\omega)$ being the conventional self-energy of the f electrons in a PAM. Correspondingly, since the c electrons are itinerant, the $\Delta(\omega)$ defined for conduction electrons is the true hybridization (with the host) while the quantity appearing in the f-Green's function, namely, $\frac{V^2}{\omega^{+}-\Delta(\omega)} = \Delta_{\rm eff}(\omega)$ is an effective hybridization for the otherwise localized f electrons. Now, a Kondo insulator assumes a low-energy Fermi-liquid form of $\Sigma_f(\omega) \sim \Sigma^{R}_{f}(0) - (1/Z-1)\omega$, which yields $\Sigma_c \overset{\omega\to 0}{\sim} ZV^2/\omega^{+}$, where $Z = (1-\partial\Sigma_f/\partial\omega)^{-1}$ is the f-electron quasiparticle weight. The $\Sigma_c(\omega)$ thus incurs a divergence at $\omega = 0$, thus leading to a gap in the corresponding spectra.

Equation (3) connects to an effective impurity model inherent to the DMFT single impurity form given by $G^{f}(\omega) = [\omega^{+} - \Sigma_f(\omega) - \Delta_{\rm eff}]^{-1}$ with $\Delta_{\rm eff}(\omega) = \frac{V^2}{\omega^{+}-\Delta(\omega)}$ being the effective hybridization seen by the f electrons and needs to be determined self-consistently. This self-consistent hybridization thus depends on the $\Delta(\omega)$, which is thus determined self-consistently within DMFT. This is therefore termed as the self-consistently determined hybridization function for the c electrons.

For a system of coupled heavy fermion layers, the layer resolved Green's functions, $G^{cc}_{\alpha\alpha}$ for the c orbitals, may be obtained through an equation of motion method, applied in real space [19]. For an N-layered system, the entire matrix of the c-Green's functions is given by the following expression:

$$\hat{G}^{cc}(\omega,\mathbf{k}^{||}) = \begin{pmatrix} \lambda_1-\epsilon(\mathbf{k}^{||}) & -t_{\perp} & 0 & \dots \\ -t_{\perp} & \lambda_2-\epsilon(\mathbf{k}^{||}) & -t_{\perp} & \dots \\ 0 & -t_{\perp} & \lambda_3-\epsilon(\mathbf{k}^{||}) & \dots \\ \vdots & \vdots & \ddots & \vdots \\ 0 & 0 & \dots & \lambda_N-\epsilon(\mathbf{k}^{||}) \end{pmatrix}^{-1}, \tag{4}$$

with $\lambda_\alpha = \omega^+ - \epsilon_{c\alpha} - \Sigma_{c\alpha}$, $\omega^+ = \omega + i\delta$, and $\mathbf{k}^{||}$ denotes the Bloch vector along the planar direction. Equation (4) assumes the existence of translational invariance along the in-plane direction. The term $\Sigma_{c\alpha}$ is the c self-energy arising due to the hybridization with the correlated f orbitals, related to the $\Sigma_{f\alpha}$ as described before. It is to be noted that the term $\Sigma_{c\alpha}$ for each layer shall be related to $\Sigma_{f\alpha}$ in the same manner as for an isolated heavy fermion layer, because we have neglected the interlayer f-orbital hopping. However, now one needs to self-consistently derive an effective Anderson impurity model and hence $\Sigma_{f\alpha}$ for each layer utilizing the full matrix structure of the local c-Green's functions (4). The above expression is not restricted to the PAM, and can be used in more general situations, e.g., if the c orbitals were correlated and thus had an intrinsic self-energy. Thus the λ_α are determined by the Hamiltonian of the αth layer. Note that the band insulator is constructed using a fictitious noninteracting localized orbital that plays no role except to hybridize with the conduction orbital and create a band gap. Thus in our calculations, the band insulators have a $\Sigma_{c\alpha}(\omega) = \frac{V_\alpha^2}{\omega^+}$. For the noninteracting metallic system, there exists no f orbitals and hence $V = 0$ thus giving $\Sigma_{c\alpha}(\omega) = 0$. For the Kondo insulators, $\Sigma_c(\omega) = \frac{V^2}{\omega^+ - \Sigma_f(\omega)}$. Therefore λ_α in Eq. (4) is given by $\omega^+ - \frac{V_\alpha^2}{\omega^+}$, ω^+ and $\omega^+ - V_\alpha^2/(\omega^+ - \epsilon_f - \Sigma_{f\alpha})$ for band insulators, metals, and Kondo insulators, respectively, with $\Sigma_{f\alpha}$ being the local f self-energy in the αth layer. Within dynamical mean-field theory, where the local approximation is valid, an impurity solver is needed to obtain the f self-energy. We have employed the local moment approach to solve the effective self consistent impurity problem.

The local c-Green's functions are given by a $\mathbf{k}^{||}$ summation of the $\hat{G}^{cc}(\omega,\mathbf{k}^{||})$ matrix. In order to avoid the numerically expensive step of summation over k_x, k_y for each frequency ω, we employ the method used in Ref. [17]. If the inverse c-Green's function matrix, $(\hat{G}^{cc})^{-1}(\omega,\mathbf{k}^{||})$ [in Eq. (4)] is denoted as $\hat{M}'$, such that $\hat{M}' = \hat{M} - \epsilon(\mathbf{k}^{||})\mathbb{I}$, $\mathbb{I}$ being a unit matrix; a similarity transformation may be then used to transform the $\hat{M}$ matrix into diagonal form, such that, $\hat{M} = \hat{S}\,\mathrm{Diag}[\Gamma_1,\Gamma_2,\ldots]\,\hat{S}^{-1}$, $\hat{S}$ being the unitary matrix that diagonalizes $\hat{M}$:

$$\hat{G}^{cc}(\omega) = \hat{\mathcal{S}}\begin{pmatrix} H[\Gamma_1] & 0 & 0 & \ldots \\ 0 & H[\Gamma_2] & 0 & \ldots \\ 0 & 0 & H[\Gamma_3] & \ldots \\ \vdots & \ldots & \vdots & \ldots \end{pmatrix}\hat{\mathcal{S}}^{-1}, \quad (5)$$

where the Hilbert transform, $H[z] = \int_{-\infty}^{\infty} d\epsilon \rho_0(\epsilon)(z-\epsilon)^{-1}$ over $\rho_0(\epsilon)$, the noninteracting planar density of states, represents the result of the $\mathbf{k}^{||}$ summation and $\hat{S}$ is the similarity transformation matrix diagonalizing M. The N eigenvalues of M are denoted by Γ_r with $r = 1,\ldots,N$. The above procedure is valid as long as the band dispersion is the same for every layer. Within layer-DMFT, each layer is treated as a single-impurity embedded within a noninteracting host. Thus the c-Green's function for the αth layer may be written as

$$G^{cc}_{\alpha\alpha}(\omega) = \sum_{r=1}^{N} S_{\alpha r}\, H[\Gamma_r]\,(S^{-1})_{r\alpha} \quad (6)$$

$$= \frac{1}{\lambda_\alpha(\omega) - \Delta_\alpha(\omega)}, \quad (7)$$

where $\lambda_\alpha(\omega) = \omega^+ - \epsilon_{c\alpha} - \Sigma_{c\alpha}$ and $\Delta_\alpha(\omega)$ is the host hybridization for the αth PAM layer and N is the total number of layers. Note that Eqs. (6) and (7) become the definition of $\Delta_\alpha(\omega)$. In all the calculations, we set the f-orbital site energy, in the αth layer, $\epsilon_{f\alpha} = -U_\alpha/2$, where U_α is the interaction strength present only on the localized f orbitals of the αth layer and the c-orbital site energy, $\epsilon_{c\alpha} = 0$, such that the chemical potential, $e_\mu = 0$, on all the layers. Thus the Luttinger sum rule implemented on the local quantities, given by $I_L = \mathrm{Im}\int_{-\infty}^{0} \frac{d\omega}{\pi}\frac{\partial\Sigma_{f\alpha}(\omega)}{\partial\omega} G^f_\alpha(\omega) = 0$, is always satisfied locally on each layer. The temperature T is set to zero.

An alternative way to approach this problem is through a Feenberg self-energy approach [29]. Consider any site on the αth layer. The $\Delta_\alpha(\omega)$ for this site may be written as a sum of self avoiding walks on the entire lattice with the lines representing hopping (intralayer given by $-t^{||}$ and interlayer by $t_\perp$), and the vertices being the site-excluded Green's functions [29]. The definition of the hybridization through equations (6) and (7) is a practical route to summing all these diagrams. The local approximation of DMFT implies that the full self-energy is momentum independent, hence the λ_r will get modified if interactions are included on the rth layer. However, since that is a local change, the diagrams for the $\Delta_\alpha(\omega)$ do not change. This implies that the definition of the host hybridization in the presence of interactions remains the same as that for the noninteracting case within DMFT, albeit computed with a new set of λ_r. Including Kondo-hole disorder on the rth layer within the coherent potential approximation (CPA) does not change this definition and is hence tantamount to redefining λ_r in the following way [28]:

$$\frac{1}{\lambda_r(\omega) - \Delta_r(\omega)} = \frac{1-p}{\gamma_r(\omega) - \Delta_r(\omega)} + \frac{p}{\gamma_{0r}(\omega) - \Delta_r(\omega)}, \quad (8)$$

where $\gamma_r(\omega) = \omega^+ - \epsilon_{cr} - \Sigma_{cr}$ represents the sites with f electrons and $\gamma_{0r}(\omega) = \omega^+ - \epsilon_{cr}$ represents the Kondo hole sites. Thus, for a given set of $\Sigma_{cr}(\omega)$, the $\lambda_r(\omega)$ and $\Delta_r(\omega)$ need to be determined self consistently by combining Eqs. (6) and (7) with Eq. (8). A practical computational procedure is the following. Step 1: guess a set of $\Delta_r(\omega)$ and use them to find λ_r from equation (8). Step 2: use these λ_r in Eqs. (6) and (7) to find a new set of $\Delta_r(\omega)$. Go back to step 1 until convergence is achieved. The obtained $\lambda_r(\omega)$ may be used to define a disorder-averaged self-energy for the rth layer as

$$\Sigma^{\mathrm{CPA}}_{cr}(\omega) = \omega^+ - \epsilon_{cr} - \lambda_r. \quad (9)$$

The self-consistent interacting impurity problem is solved here using the local moment approach (LMA). The LMA is a diagrammatic perturbation based approach, built around the two broken-symmetry, local moment solutions ($\mu = \pm|\mu_0|$) of an unrestricted Hartree-Fock mean-field approximation. Spin-flip dynamics are subsequently built in through an infinite-order resummation of a specific class of diagrams that embody transverse spin-flip processes. A key ingredient of LMA is the symmetry restoration condition which is equivalent to imposing adiabatic continuity to the noninteracting limit, and is hence crucial to recovery of Fermi liquid behavior and the emergence of a low-energy scale. Any violation of this condition signals a quantum phase transition to another phase such as a local moment phase. By construction, the scope of

LMA is limited to investigations of Kondo physics, and a generalization of the method to ordered phases or cluster problems is not straightforward. Moreover, the practical implementation of the resummation is through a random phase approximation, which introduces certain undesirable features in the transverse spin polarization propagator (see Ref. [30]). Nevertheless, the LMA has been found to benchmark excellently against numerical renormalization group (NRG) [31], and Bethe ansatz for the SIAM and the Kondo problem, respectively [30]. It has henceforth been employed in studies on Kondo insulators and heavy fermion systems [32–35]. It has also been used in studying specific cases of impurity systems with many orbitals, the pseudogap Anderson model and the gapped Anderson impurity model [36]. The study on the soft gap Anderson model has also been compared to NRG in Ref. [37]. The extension to finite disorder may be found in Ref. [28]. We combine LMA, CPA, and the inhomogeneous DMFT [19] to explore the effect of disorder and interactions in layered-PAM systems.

At this point it is worth mentioning that although the DMFT systematically incorporates the dynamical effects of strong correlation by its construction, it ignores the feedback of the spatially nonlocal intersite correlations into single particle quantities in either the charge channel (nearest-neighbor) or the spin channel (exchange). Particularly, here, in the context of heavy fermion systems the investigation of the competition between the Kondo effect and the Rudderman-Kittel-Kasuya-Yosida (RKKY) interaction is therefore beyond the scope of DMFT. The Coherent Potential Approximation (CPA) is also a single site approximation. In the present context, the CPA equations lead to a self-consistently obtained disorder averaged f-electron self-energy, $\Sigma_f^{\rm CPA}(\omega)$ that is equal for all sites. Hence the CPA too cannot describe physical scenarios stemming from beyond mean-field disorder effects. For example, effects like Anderson localization or non-Fermi liquid physics that occur due to a distribution of Kondo scales cannot be explored within this approach. Our investigation is therefore a minimal model that may look at the some effects of disorder in layered systems.

III. RESULTS

We have explored the proximity effects of a Kondo hole-disordered heavy fermion layer in thin films, by studying geometries where the substitutionally disordered Kondo insulator is in proximity to several clean interacting or noninteracting layers. Before we delve into results obtained using the numerical implementation of the local moment approach within inhomogeneous DMFT, we present a few general results that are exact within this framework of layered systems.

A. Analytical results for a few special cases

Using the equations detailed in Sec. II, it is easy to obtain closed-form expressions for the Green's functions in certain simple cases. We present and discuss a few results for a noninteracting layered system, a bilayer and a trilayer system.

1. Non-interacting case

For N-identical layers the matrix on the right-hand side of Eq. (4) has the structure of a symmetric tridiagonal Toeplitz matrix [38]. The complete eigenspectrum and corresponding eigenvectors for such a matrix are known in closed form [38], and hence may be used in combination with Eq. (4) to find the exact Green's functions for the nth layer of a system of N identical noninteracting metallic layers (see also Ref. [39]). The density of states at a fixed ω as a function of layer-index becomes

$$A_n(\omega) = \frac{2}{N+1}\sum_{m=1}^{N}\sin^2\left(\frac{mn\pi}{N+1}\right)\rho_0\left(\omega+2t_\perp\cos\frac{m\pi}{N+1}\right). \tag{10}$$

With the replacement of ω by $\omega - V^2/\omega$ in the above equation, the result describes N identical noninteracting band-insulators also.

$A_n(\omega)$, shown in Fig. 1, exhibits oscillatory behavior for all ω values except $\omega = 0$ where a monotonic decay is observed. These well-known surface Friedel oscillations arise because the Fermi surface of the infinite metallic system has been perturbed by the presence of terminal surfaces [19,10].

2. Bilayer systems: general considerations

For a bilayer system, the Green's functions are given by

$$G_{11}(\omega) = a\,H[\Gamma_+] + b\,H[\Gamma_-], \tag{11}$$

$$G_{22}(\omega) = a'\,H[\Gamma_+] + b'\,H[\Gamma_-], \tag{12}$$

where

$$\Gamma_\pm = \frac{1}{2}(\lambda_1+\lambda_2 \pm \sqrt{(\lambda_1-\lambda_2)^2+4t_\perp^2}),$$
$$\lambda_r = \omega^+ - \epsilon_c - \Sigma_{cr}(\omega), \quad r = 1,2, \tag{13}$$

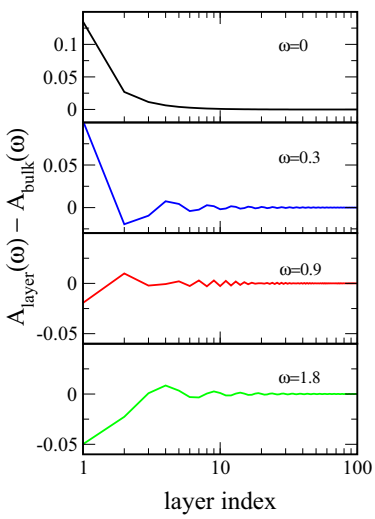

FIG. 1. (Color online) The change in layer density of states (compared to the bulk) as a function of layer index, for various frequencies. The result was obtained using Eq. (10) for a system of 500 layers. The bare density of states for each layer $\rho_0(\epsilon)$ is chosen to be of semielliptic form, $\rho_0(\epsilon) = (\sqrt{1-\epsilon^2/t_{||}^2})/(2\pi t_{||})$.

$$a = \frac{\Gamma_+ - \lambda_2}{\Gamma_+ - \Gamma_-} \quad \text{and} \quad b = \frac{\lambda_2 - \Gamma_-}{\Gamma_+ - \Gamma_-}, \tag{14}$$

$$a' = -\frac{\lambda_1 - \Gamma_+}{\Gamma_+ - \Gamma_-} \quad \text{and} \quad b' = \frac{\lambda_1 - \Gamma_-}{\Gamma_+ - \Gamma_-}, \tag{15}$$

and $H[z]$ represents the Hilbert transform with respect to the noninteracting layer density of states. These equations may now be analyzed for a few specific cases.

3. A clean Kondo insulator-metal bilayer system

As a first application of Eqs. (11) and (12), we consider a Kondo-insulator-metal interface. The paramagnetic Kondo insulator is just a renormalized band insulator, hence in the particle-hole symmetric limit, $\epsilon_c = 0$ and $\Sigma_c(\omega) = V^2/(\omega^+ - \epsilon_f - \Sigma_f)$. In the low-frequency limit, the Fermi-liquid form of the f self-energy may be used to get $\Sigma_c \overset{\omega\to 0}{\sim} ZV^2/\omega^+$, where $Z = (1 - \partial\Sigma_f/\partial\omega)^{-1}$ is the f-electron quasiparticle weight. Thus $\lambda_1 = \omega^+ - ZV^2/\omega^+$ for the Kondo insulator and $\lambda_2 = \omega^+$ for the noninteracting metal. Given these, the c-spectral functions $A_l(\omega) = -\mathrm{Im}G^c_{ii}(\omega)/\pi$ for the Kondo insulator ($i = 1$, $l = KI$) and metal ($i = 2$, $l = M$) layers in the low-frequency limit are given by

$$A_{\mathrm{KI}}(\omega) \overset{\omega\to 0}{\sim} \left(\frac{\omega t_\perp}{ZV^2}\right)^2 \rho_0\left[\omega\left(1 + \frac{t_\perp^2}{ZV^2}\right)\right] + \left[1 - \left(\frac{\omega t_\perp}{ZV^2}\right)^2\right]\rho_0\left[\omega\left(1 - \frac{t_\perp^2}{ZV^2}\right) - \frac{ZV^2}{\omega}\right], \tag{16}$$

$$A_M(\omega) \overset{\omega\to 0}{\sim} \left[1 - \left(\frac{\omega t_\perp}{ZV^2}\right)^2\right]\rho_0\left[\omega\left(1 + \frac{t_\perp^2}{ZV^2}\right)\right] + \left(\frac{\omega t_\perp}{ZV^2}\right)^2 \rho_0\left[\omega\left(1 - \frac{t_\perp^2}{ZV^2}\right) - \frac{ZV^2}{\omega}\right]. \tag{17}$$

From the above expressions, we see that the presence of interlayer coupling ($t_\perp > 0$) leads to a linear mixing of the Kondo-insulator and metallic layer spectra in all layers. In $A_{\mathrm{KI}}(\omega)$, the first term contributes a quadratically vanishing spectral weight into the hybridization gap, while the second-term leads to the usual gapped spectrum of the Kondo insulator. In $A_M(\omega)$, the first term implies that the spectrum of the noninteracting metal is strongly renormalized by the proximity to the Kondo insulator, and a Kondo resonance like feature must emerge in the vicinity of the Fermi level. The second term is gapped at the Fermi level, but should lead to a step like feature at $\omega \sim ZV^2$. Thus the metallic states tunnel into the gap of the Kondo insulator giving rise to a quadratically vanishing gap, while the strongly correlated Kondo insulator tunnel into the noninteracting metal leading to strong renormalization of the noninteracting spectrum. In the Kondo insulator, the f-electron spectrum is related to the c-electron spectrum through $A^f_{\mathrm{KI}}(\omega) = (Z^2V^2/\omega^2)A_{\mathrm{KI}}(\omega)$ in the limit $\omega \to 0$. Due to the tunneling of the metallic states into the Kondo insulator, the f spectrum thus becomes gapless. These proximity effects are quite general and only assume a linear expansion in frequency of the real part of the f self-energy. Similar results have been observed numerically in a recent study on a single Kondo insulator embedded in a three-dimensional noninteracting metallic host [20] and in a theoretical analysis of the surface density of states of heavy fermion materials [24]. This physical scenario of "Kondo proximity effect" was used to qualitatively explain the experimental surface spectra of $CeCoIn_5$ reported by Aynajian *et al.* [40].

4. A clean Kondo insulator-band insulator bilayer system

Next, we consider a Kondo-insulator-band-insulator interface. For the band insulator, $\lambda_2 = \omega^+ - V^2/\omega^+$. Thus the spectral functions are again given by a linear mixing of the Kondo and the band insulator spectra. A low-frequency analysis similar to the one carried out above for the Kondo insulator-metal system leads to the following. The gap in the Kondo insulator is well known to be substantially reduced compared to the band insulator due to the exponentially small quasiparticle weight factor Z arising in the strong-coupling limit. Thus, from our analysis, we see that the Kondo insulator spectrum close to the Fermi level remains almost unchanged. However, in the frequency region where the band insulator had a gap, but the Kondo insulator had states, a quadratically vanishing spectral weight tunnels in from the Kondo insulator layer into the band insulator.

5. A dirty Kondo insulator-metal bilayer system

In this section, we consider, in detail, a substitutionally disordered-Kondo-insulator interfaced with a noninteracting metal. The random substitution of f sites in the Kondo insulator-layer leads to Kondo hole disorder, which is known to lead to an impurity band at the Fermi level [41,42]. Specifically, λ_1 becomes complex because of the static contribution to the self-energy from scattering by impurities [28]. Thus $\lambda_1 = \omega^+/Z + i\Gamma_0$, where Z is the local f-electron quasiparticle weight and $\Gamma_0 = -\mathrm{Im}\Sigma_c^{\mathrm{CPA}}(0)$ is the scattering rate at the Fermi level. In a previous paper [28], we showed that Σ_c^{CPA} may be related to Σ_c through a cubic equation if $\rho_0(\epsilon)$ has a semielliptic form that corresponds to an infinite-dimensional Bethe lattice. This equation, if used for a single isolated Kondo insulator, yields that

$$\Sigma_c^{\mathrm{CPA}}(0) = -it_{||}\frac{1-p}{2\sqrt{p}}. \tag{18}$$

Thus, at the Fermi level, the conduction electrons acquire a self-energy that is nonanalytic in the concentration of Kondo holes, p. It was also shown in Ref. [42] that the f electron self-energy acquires a $1/\sqrt{p}$ dependence when $p \to 0$. However, in the presence of interlayer coupling, Γ_0 becomes a complicated function of $t_\perp$ and $t_{||}$ and we have not been able to find a simple closed form expression like Eq. (18) for the bilayer case. Nevertheless, numerical calculations lead us to the conclusion that Γ_0 does retain the same form as the isolated layer case.

Our natural focus is on the strong coupling regime of the Kondo insulator, where the quasiparticle weight becomes exponentially small, i.e., $Z \to 0$. In such a situation, and with $\lambda_1 = \omega^+/Z + i\Gamma_0$ and $\lambda_2 = \omega^+$, the values of $\Gamma_\pm$ in Eq. (13) may be simplified to

$$\Gamma_\pm \overset{Z\to 0}{\longrightarrow} \tfrac{1}{2}\left(\lambda_1 \pm \sqrt{\lambda_1^2 + 4t_\perp^2}\right). \tag{19}$$

The coefficients of the Hilbert transforms in Eqs. (11) and (12) are given by

$$a \to \frac{\Gamma_+}{\sqrt{\lambda_1^2 + 4t_\perp^2}} \quad b \to \frac{-\Gamma_-}{\sqrt{\lambda_1^2 + 4t_\perp^2}},$$
$$a' = b \quad \text{and} \quad b' = a\,. \tag{20}$$

These equations are quite easy to analyze at the Fermi level ($\omega = 0$). In fact, the results from this analysis do not assume strong coupling, because if we substitute $\omega = 0$ in the above expressions, the quasiparticle weight does not appear in them. Hence the following results are valid for any coupling strength. At the Fermi level, the eigenvalues are given by

$$\Gamma_\pm = \frac{i}{2}\left(\Gamma_0 \pm \sqrt{\Gamma_0^2 - 4t_\perp^2}\right). \tag{21}$$

Γ_0 is a monotonically decreasing function of the Kondo hole concentration [see equation (18)] and hence in the dilute limit ($p \to 0$), the eigenvalues will be purely imaginary; with increasing p, $\Gamma_\pm$ become degenerate at $\Gamma_0 = 2t_\perp$, which translates to a specific concentration, p_d. In general, p_d is a complicated function of Γ_0. However, we have numerically verified that when the ratio $t_\perp/t_{||} \ll 1$, Eq. (18) can be used as an estimate of p_d for multi-layer systems. For such a regime $p_d = (\sqrt{1 + (2t_\perp/t_{||})^2} - 2t_\perp/t_{||})^2$. For $p > p_d$, the two eigenvalues have the same imaginary part but differ in the real part. It turns out that the density of states at the Fermi level can be easily obtained in two limits: the dilute limit ($p \to 0$) and the degenerate limit ($\Gamma_0 = 2t_\perp$ or $p = p_d$). We proceed to obtain these.

In the dilute limit, $\Gamma_0 \gg t_{||}, t_\perp$, so $\Gamma_+ \to i(\Gamma_0 - t_\perp^2/\Gamma_0)$ and $\Gamma_- \to it_\perp^2/\Gamma_0$. For purely imaginary arguments ($z = i\eta$), the Hilbert transform with respect to a semi-elliptic density of states may be written in closed form as

$$\mathcal{H}(i\eta) = \int \frac{\rho_0(\epsilon)}{i\eta - \epsilon} = -\frac{2\,i}{t_{||}}[\sqrt{1 + \bar{\eta}^2} - \bar{\eta}], \tag{22}$$

where $\bar{\eta} = \eta/t_{||}$. So the Hilbert transform is also purely imaginary, which can be expected in the particle-hole symmetric limit. Using the above Hilbert transform result and the simplification of the eigenvalues in the dilute limit, the density of states of the Kondo insulating layer and the noninteracting metallic layer are given by [to $\mathcal{O}(1/\Gamma_0^2)$]

$$A_{\rm KI}(\omega = 0) \xrightarrow{p \to 0} \frac{1}{\pi\Gamma_0}\left(1 - \frac{2t_\perp^2}{\Gamma_0 t_{||}}\right), \tag{23}$$

$$A_M(\omega = 0) \xrightarrow{p \to 0} \frac{2}{\pi t_{||}}\left(1 - \frac{t_\perp^2}{\Gamma_0 t_{||}} + \frac{t_\perp^2}{\Gamma_0^2}\right). \tag{24}$$

Note that in all the equations above and below, $A_{\rm KI}(\omega)$ denotes the c-electron spectral function of the Kondo insulator. The above equations reveal the proximity effect of disorder on the two layers. In the absence of interlayer tunneling, the impurity band in the Kondo insulator grows as $\sqrt{p}$ with increasing Kondo hole substitution (since $\Gamma_0 \sim 1/\sqrt{p}$ in the dilute limit); and the metallic layer has a fixed density of states ($= 2/(\pi t_{||})$) at $\omega = 0$. When $t_\perp$ is turned on, the impurities introduced in the Kondo insulating layer affect the density of states of the noninteracting clean metallic layer, and the relative change in the density of states with respect to the isolated layers ($t_\perp = 0$) case is $\sim\sqrt{p}$ for both layers.

In the degenerate limit, $\Gamma_0 = 2t_\perp$, the eigenvalues are degenerate, and Eqs. (11) and (12) cannot be used. We revert back to the basic equation (5) and after a bit of algebra, obtain the density of states of the two layers as

$$A_{\rm KI}(\omega = 0) \xrightarrow{p = p_d} \frac{2}{\pi t_{||}} \frac{\left(t_r - \sqrt{1 + t_r^2}\right)^2}{\sqrt{1 + t_r^2}}, \tag{25}$$

$$A_M(\omega = 0) \xrightarrow{p = p_d} \frac{2}{\pi t_{||}} \frac{1}{\sqrt{1 + t_r^2}}, \tag{26}$$

where $t_r = t_\perp/t_{||}$ is the ratio of the interlayer to intralayer hopping. We have seen that the metallic layer acquires a Kondo resonance at the Fermi level due to the proximity to the Kondo insulator. Since in the concentrated limit ($p \to 1$), the entire system simply becomes a noninteracting metallic bilayer, the density of states must approach the value of $\rho_0(t_\perp)$. It can also be shown that, the $A_M(\omega = 0) > \rho_0(t_\perp)$. This implies that both the metallic layer and the Kondo insulating layer experience a monotonic change in the density of states with increasing Kondo hole concentration; the Kondo insulating layer steadily transforming into a single-impurity system.

6. *Symmetric trilayer systems*

Another class of systems, for which closed form expressions may be readily obtained is a set of three layers in which the outer two layers are identical in all respects while the middle layer is different. The c-Green's function for such a system (denoted by 1-2-3) is given by

$$G_{11}(\omega) = G_{33}(\omega) = \tfrac{1}{2}H[\lambda_1] - t_\perp^2(a\,H[\Gamma_+] + b\,H[\Gamma_-]), \tag{27}$$

$$G_{22}(\omega) = a'\,H[\Gamma_+] + b'\,H[\Gamma_-], \tag{28}$$

where

$$\Gamma_\pm = \frac{1}{2}(\lambda_1 + \lambda_2 \pm \sqrt{(\lambda_1 - \lambda_2)^2 + 8t_\perp^2}),$$
$$\lambda_r = \omega^+ - \epsilon_c - \Sigma_{cr}(\omega),$$
$$a = \frac{1}{(\lambda_1 - \Gamma_+)(\Gamma_+ - \Gamma_-)} \quad \text{and}$$
$$b = \frac{-1}{(\lambda_1 - \Gamma_-)(\Gamma_+ - \Gamma_-)},$$
$$a' = -\frac{\lambda_1 - \Gamma_+}{\Gamma_+ - \Gamma_-} \quad \text{and} \quad b' = \frac{\lambda_1 - \Gamma_-}{\Gamma_+ - \Gamma_-}.$$

For the trilayer system, if the layers are uncoupled ($t_\perp = 0$) then the Green's functions should be simply given by $G_{ii}(\omega) = H[\lambda_i]$. In order to approach the uncoupled layers limit, in the equations above, the limit of $t_\perp \to 0$ must be taken with care. We have investigated the symmetric trilayer system in several situations, that are similar to the ones discussed for the bilayer system. One of these is a Kondo insulator, which could be clean or substitutionally Kondo hole disordered, sandwiched between two metallic or band-insulating layers. The conclusions reached in such cases were found to be qualitatively very similar to those in the bilayer systems,

hence we now proceed to larger systems and investigate the penetration of disorder into several clean, noninteracting or interacting layers. In the next section, we discuss full numerical solutions using the formalism described in Sec. II.

B. Numerical results

It is evident that the spectral changes in the c- and f-electron Green's functions are a combined effect of the three physical parameters in the problem, namely: (i) interlayer hopping $t_\perp$, (ii) interaction U, and (iii) Kondo hole concentration (p). In order to disentangle the sole effect of disorder from the results, we first discuss briefly the noninteracting and clean layered systems. Then, we add interactions and note the combined effect of inter layer coupling and interactions. Finally, we add disorder and by comparing the obtained spectra to those of the nondisordered case, we isolate the proximity effects of disorder, which represents the main objective of this paper. We study three different cases, with a single substitutionally disordered Kondo insulator layer next to (a) several band insulator, (b) several uncorrelated metal, and (c) several clean Kondo insulator layers. These three cases will be referred to as disordered Kondo insulator-band insulator, disordered Kondo insulator-metal and disordered Kondo insulator-Kondo insulator, respectively. A schematic of the geometries is shown in Fig. 2. The number of clean layers has been varied from 1 to 11. The clean metals are just $U = 0$ layers with a simple tight-binding Hamiltonian. In the disordered Kondo insulator-Kondo insulator case, all the Kondo-insulating layers including the disordered layer have the same U and V. All of the numerical results have been obtained by using a semi-elliptic bare density of states for each layer, namely, $\rho_0(\epsilon) = (\sqrt{1-\epsilon^2/t_{||}^2})/(2\pi t_{||})$, with $t_{||} = 1$ as the unit of energy. We begin this section by considering the effects of $t_\perp$ only, in a clean, noninteracting, f-conduction-electron system,

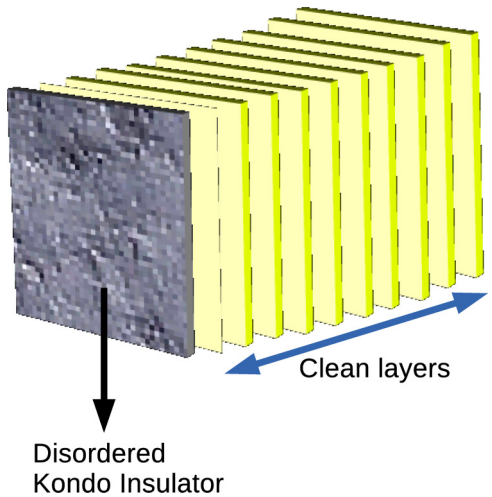

FIG. 2. (Color online) Schematic of the geometry considered in this work. While the boundary layer is chosen to be a dirty Kondo insulator, the proximal layers are clean. Three distinct possibilities for these clean layers have been investigated, namely: band-insulators, metals, or Kondo insulators.

interfaced with several noninteracting metals or several other noninteracting f-conduction-electron systems.

1. *Effects of interlayer hopping: $t_\perp \neq 0$, $U = 0$, $p = 0$*

In Fig. 3, the layer-resolved c-spectra for a single band insulator coupled to 11 metallic layers is shown. Since the entire system is particle-hole symmetric, we choose to display only the $\omega > 0$ spectrum on a logarithmic energy scale. The spectrum for an isolated band insulator layer is shown as a dashed line in both panels. From the top panel of Fig. 3, we observe that the presence of $t_\perp$ between a metallic layer next to a band insulator leads to the tunneling of metallic states into the otherwise large hybridization gap of the band insulator. We had predicted earlier, in Sec. III A 4, that the presence of $t_\perp$ leads to a quadratic rounding off of the band insulator band edge, which is evident when compared with the hard band edge of the isolated layer's hybridization gap (dashed line). The multiple Friedel oscillations due to a nonzero $t_\perp$ are also visible in Fig. 3. Although the predictions were exact for a bilayer system, the layer resolved spectra follow the same qualitative changes in this multi-layered system. These oscillations naturally attenuate sharply in the layers that lie far from the boundaries. However, for all the finite-layer systems that we have studied, these oscillations are present. Nevertheless, as Freericks *et al.* discussed in Ref. [19], and also found by us, the amplitude of these oscillations in the surface layers become frozen-in once the system becomes large

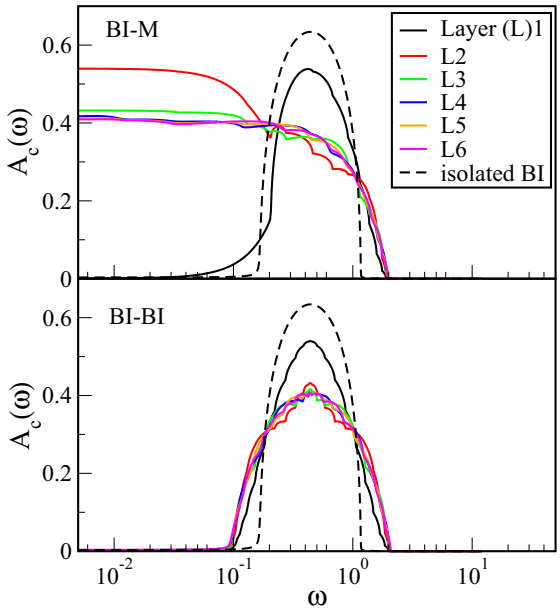

FIG. 3. (Color online) Spectral density of the c electrons in the presence of nonzero interlayer coupling for a single band insulator layer (L1) at one end of an 11-layer (L2-L12) metallic system (top) and a single band insulator at one end of an 11-layer band insulating system (bottom) plotted on a logarithmic energy scale. The model parameters are $t_\perp = 0.5$, $U = 0$, $V = 0.44$. Note that only $\omega > 0$ part of the spectrum is displayed, which is sufficient because of particle hole symmetry in the present problem. The spectrum of an isolated band insulator layer is shown as a dashed line to contrast the changes brought about because of the additional layers.

($\gtrsim$10 layers in practice). Next, we explore the combined effect of interlayer coupling and interactions.

2. Combined effect of interlayer hopping and interactions: $t_\perp \neq 0$, $U \neq 0$, $p = 0$

In Fig. 4, we show the layer-resolved c spectra for a single Kondo insulator and 11 metallic layer system (top panel) and a single Kondo insulator and 11-band insulator layer system (bottom panel). In this bottom panel, due to the presence of finite density of states in the proximal Kondo insulator, we see that the c spectra of the second neighboring band insulator layer acquires a quadratic rounding off around the band edge. The farther band insulator layers are however inert to these effects.

The top panel of Fig. 4 shows that, for a metallic layer adjacent to a Kondo insulator, the proximity effect results in a Kondo-like resonance at the Fermi level of the otherwise noninteracting metal. This is consistent with the numerical renormalization group results of Peters *et al.* on Kondo superlattices and the emergent Kondo proximity effect as discussed in Ref. [20]. An insight into this can already be realized by looking at the analytical predictions of Sec. III A 3.

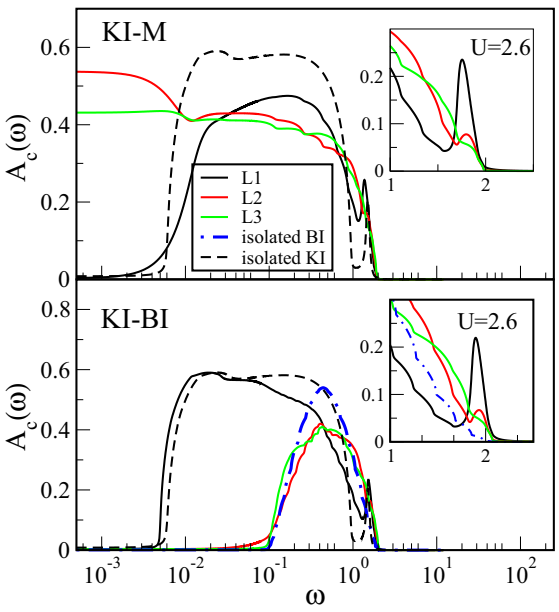

FIG. 4. (Color online) Layer-resolved spectral function for the c electrons due to nonzero interlayer hopping and interactions. A single Kondo insulator layer (L1) is coupled to an 11-layer metallic system (top) and an 11-layer band insulating system (bottom). The spectra for the nearest (L2) and second nearest (L3) metallic (top), and the band insulator (bottom) are shown. For both panels interlayer hopping, $t_\perp = 0.5$ and c-f hybridization is set to $V = 0.44$ for both the Kondo insulators and the band insulators, Coulomb repulsion in the Kondo insulating layer $U = 1.7$ in the main panels and $U = 2.6$ in both insets. For comparison, the c-DOS of an isolated Kondo insulator and an isolated band insulator is also shown as (black) dashed (top and bottom) and (blue) dashed-dotted lines (bottom), respectively. The insets show the Hubbard bands that emerge as a result of their proximity to the coupled Kondo insulator. This effect is visibly detectable only until the second nearest-neighbor layer.

Thus the low-energy analysis of Sec. III A although derived for bilayer (Kondo insulator-band insulator and Kondo insulator-metal) systems, remain robust even when the number of band insulator or metal layers is increased. Proximity to a strongly interacting Kondo insulator induces changes not only at low energies such as the Kondo scale, but also at high energies such as Hubbard bands. The adjacent noninteracting band-insulating or metallic layers also acquire minute Hubbard bands indicating the tunneling of electron correlations into the noninteracting layers. Similar effects occur even in bulk heavy fermions, modeled by the periodic Anderson model, where although the U is present only for f electrons, the mixing between c and f electrons through the hybridization produces Hubbard bands in the spectrum of the conduction band electrons. Whether the single Kondo insulator is coupled to band-insulating or metallic layers, these high energy proximity effects are the same, which is evident from the insets of Fig. 4. Now we proceed to explore the spectral modifications induced in the layer resolved spectra when we introduce Kondo holes in the boundary Kondo insulator layer.

3. Effects of Kondo hole disorder in the boundary layer

The effects of Kondo-hole disorder in the bulk PAM have been extensively investigated [25,28,41,42]. It is well known that there is a crossover from coherent lattice behavior to incoherent single-impurity behavior as the disorder p changes from zero to one [25,28]. Such a crossover is reflected in all physical quantities, including resistivity, thermopower and density of states. For layered systems, the range and extent of disorder effects may be quantified through a measurement of integrated spectral weight difference in a given frequency interval $|\omega| \leqslant \lambda$. We define $\chi_\nu(p, p_0; \alpha; \lambda)$, as the spectral weight difference of the αth layer, computed through

$$\chi_\nu(p; p_0; \alpha; \lambda) = \int_{-\lambda}^{\lambda} d\omega \, |A(p; \{U_\beta\}; \alpha; \omega) - A(p_0; \{U_\beta\}; \alpha; \omega)| \quad (29)$$

for a set of fixed interaction strengths $\{U_\alpha\}$. Here, $\nu = c/f$ and $A(p; \{U_\beta\}; \alpha; \omega) = -\mathrm{Im}G_\alpha(p; \{U_\beta\}; \omega)/\pi$ is the spectral function of the αth layer's when the Kondo hole concentration is p. Physically, this quantity represents the extent to which the layer density of states changes when disorder goes from p_0 to p or vice versa when all other parameters are fixed. We have employed $n_c = 1$ and $n_f = 1$ for an isolated Kondo insulator layer. We have observed that for an isolated layer, the spectral weight difference between the disordered and the clean case integrated over all frequencies [with the cutoff $\lambda \to \infty$ in Eq. (29)] rises rapidly as a function of increasing p and roughly saturates at the "maximally random" concentration of $p \sim 0.5$ The spectral weight difference at $p \sim 0.5$ is large when compared with either clean case ($p = 0$) or the $p \to 1^-$ single-impurity case. Hence we choose a fixed disorder $p = 0.5$ on the boundary layer in all of our subsequent discussion, unless otherwise mentioned. The rest of the layers are chosen to be clean.

With the experimental realizations of $CeIn_3/LaIn_3$ superlattices [23] and thin films of nonmagnetic Yb substituted into $CeCoIn_5$ [26], the possibility of having an interface between a Kondo hole disordered layer and a clean layer cannot be

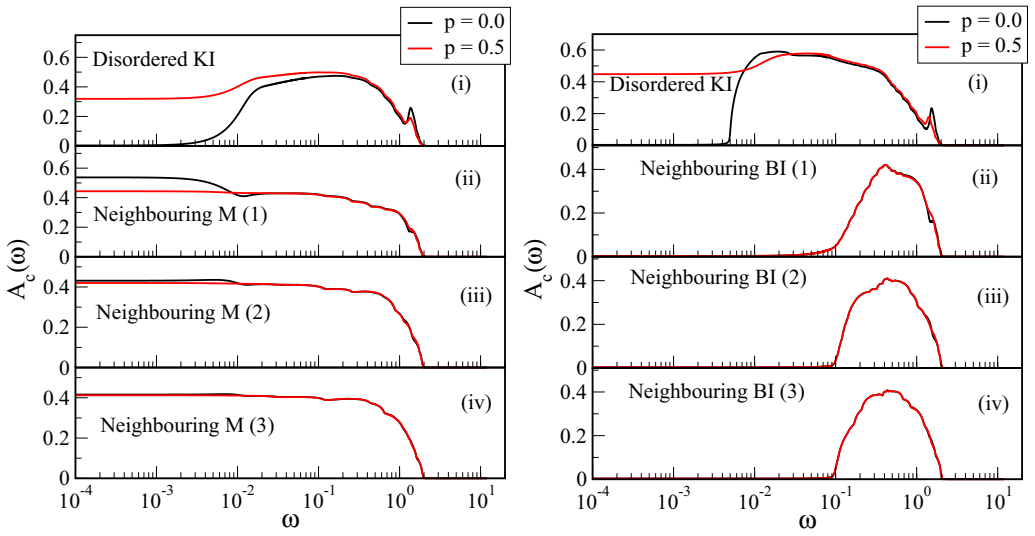

FIG. 5. (Color online) The c-electron spectra of the respective layers as denoted in the panels for a single disordered Kondo insulator interfaced with an 11-layer metallic (M) (left) or band insulating (BI) (right) system for a clean ($p = 0$) (solid black) and a disordered ($p = 0.5$) Kondo insulating (KI) layer (solid red). For the disordered Kondo insulator, this represents the CPA average of $-\Im G_{\rm CPA}/\pi$. The model parameters are $t_\perp = 0.5$, $V = 0.44$, $U = 1.7$.

ignored. We focus on the following questions: how does the random dilution of f electrons in a single Kondo insulator boundary layer (see schematic Fig. 2) affect the dynamics of the electrons in the adjoining clean layers? How far do the disorder effects penetrate? And does this range get enhanced or suppressed by the presence of interactions?

In order to answer these questions, we therefore investigate the interface of a single disordered Kondo insulator and several clean layers that could be noninteracting metals or band-insulators or strongly interacting Kondo insulators. We start our discussion with a system of 12 layers where the boundary layer is a disordered Kondo insulator and the rest of the layers are noninteracting metals. We refer to this as a disordered Kondo insulator-metal system. The proximity of a clean Kondo insulator to a metal leads to (i) a quadratic band bending at the Kondo hybridization band edge of the Kondo insulator layer and (ii) appearance of a Kondo resonance and a strongly renormalized low energy spectra induced by the "Kondo proximity effect." This has already been discussed earlier for a bilayer Kondo insulator-metal interface. In the presence of disorder, it is well known that Kondo holes introduce an impurity band in the center of the Kondo hybridization gap [41]. This impurity band then fills up the gap with increasing disorder concentration, leading to a continuum of metallic states spanning the entire gap. This observation holds here too as seen in the panel (i) of Fig. 5. This phenomenon due to Kondo holes manifests itself in both the CPA averaged c-electron spectra and the local (impurity) f-electron spectra of the disordered Kondo insulator (not shown here). Additionally, the Hubbard bands get depleted due to the presence of Kondo holes. The important aspect however, is that these disorder effects do not just remain confined to the disordered layer but also penetrate into the neighboring clean layers depicted in the lower panels of Fig. 5. Disorder in fact destroys the proximity effects of interactions. The Kondo resonance in the adjoining metallic layer at zero disorder appreciably reduces in intensity when the Kondo hole concentration, p is 0.5 and tends to disappear as p increases. This is more clearly visible from Fig. 6. The low-energy spectra of the farther neighbors also acquire visible low-energy spectral changes that evolve with change in disorder concentration, tending to crossover to the noninteracting limit of a clean metal/metal interface, as seen from Fig. 6. The tiny Hubbard bands in the noninteracting layers also disappear

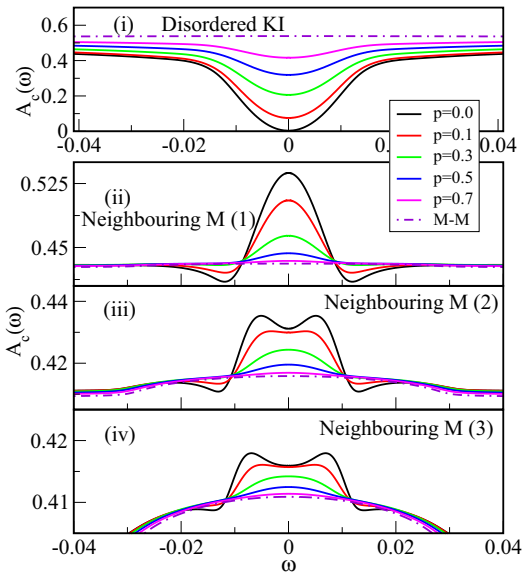

FIG. 6. (Color online) Spectral evolution at low energies for the disordered Kondo insulator (i) and the proximal clean metals [(ii)–(iv)]. A system of a single disordered Kondo insulator and 11 clean metallic layers is used. The respective layer-resolved metallic spectra corresponding to a 12 layer metal-metal (M-M) system is also shown for comparison. The model parameters are the same as used in Fig. 5

with increasing disorder. This can be expected qualitatively because introducing Kondo holes implies that sites with f orbitals in the boundary layer are randomly being replaced by noninteracting sites, hence the effects of interactions should get mitigated not only in the layer but also in the adjoining layers.

The penetration of Kondo holes into proximal band insulating layers is however different (than the proximity to metals discussed above). The exponentially larger noninteracting hybridization gap of the proximal band insulators prohibit electrons from tunneling into the insulating gap. Thus disorder-induced spectral changes in proximal band insulators remain confined to the band edges and the high energy Hubbard bands. To this end, we refer back to our discussion on the Kondo insulator/band insulator bilayer interface in Sec. III A 4. There we realized that, around the band edges of the proximal band insulator, where the Kondo insulator has available states, a quadratic band bending would occur owing to the interlayer coupling. If the clean layers are also interacting Kondo-insulators, the proximity effects of disorder span over all frequency scales, from the universal, hybridization gap scale to the nonuniversal, Hubbard bands. This shall be discussed now.

The boundary layer metallic states introduced by Kondo hole disorder now tunnel into the adjoining Kondo insulator, causing the quadratic bending of the gap in the adjacent layer (see Fig. 7). This tunneling effect does propagate into the further layers, but is attenuated by the ω^2 factor and is hence too small to be observed. The mechanism of penetration of the Kondo hole disorder-induced metallic states from the disordered Kondo insulator to the coupled clean Kondo insulator is thus physically very similar to that of a clean metal interfaced with a clean Kondo insulator [see Eqs. (16) and (17)].

In the disordered Kondo insulator layer, spectral weight transfer occurs across all scales. It is well known that Kondo hole substitution results in a coherent lattice to an incoherent single-impurity crossover. This manifests in the transfer of weight from high-energy Hubbard bands to the Kondo resonance. Concomitantly, the hybridization experienced by the interacting sites in the boundary layer crosses over to a featureless noninteracting lineshape. The adjacent layers get strongly affected by these changes and the spectral weight transfer occurs across all energy scales in the nearest-neighbor Kondo insulator as well. The Hubbard bands in the second layer too acquire an explicit Kondo hole induced depletion. Although there exists no explicit interlayer f-c hybridization the f electrons in the clean layers get strongly influenced by the presence of Kondo holes in its adjacent layer. This is because the f-e$^-$s of the proximal clean layers see a self-consistently determined layer dependent host hybridization function, $S(\omega)$, as can be seen from Eq. (7). We now quantify the spectral weight transfers focusing on the role of interactions in the proximity effects of disorder.

As explained earlier, the spectral weight difference between the spectra, with and without disorder, integrated in a given frequency interval, represents one measure of the proximity effect of disorder. We have chosen two frequency intervals: (i) a "low-frequency" interval defined by $|\omega| \leqslant \Omega_{\rm BI}$, where $\Omega_{\rm BI} = \frac{1}{2}(-t_{||} + \sqrt{t_{||}^2 + 4V^2})$, represents the hybridization gap edge of an isolated band insulator and (ii) the entire frequency range. This classification into low frequencies and all frequencies is done to emphasize that the low-frequency spectral changes could be tiny [$\sim \omega_L \rho_0(0)$, which is exponentially small in strong coupling] but affect low-temperature properties, especially transport, in a major way. The spectral changes over *all* frequencies will show up in photoemission and optical properties measurements, and hence are important from a different perspective. Since the Kondo holes are introduced only in the boundary layer, the spectral weight transfers would be maximal there. Moving away from the disordered Kondo insulator layer, the changes in the spectra due to the boundary layer disorder must decrease. Indeed, this expectation is borne

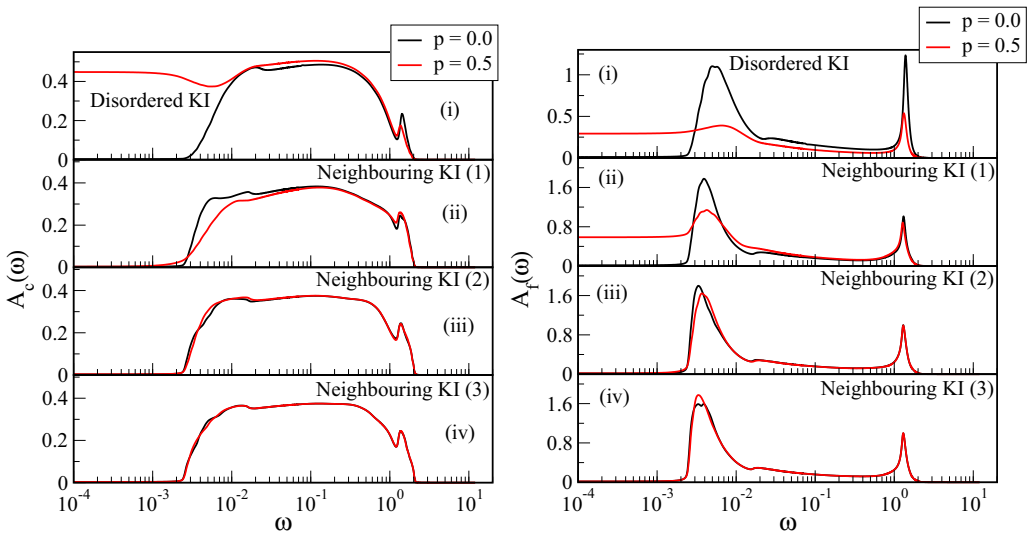

FIG. 7. (Color online) (Left) The layer resolved c-electron spectra of a single disordered Kondo insulator coupled to 11 clean Kondo insulating (KI) layers. The respective layers are denoted in the panels. (Right) The same for the CPA averaged f electrons of the disordered Kondo insulator and the interacting f electrons of the clean Kondo insulators. The parameters used are $t_\perp = 0.5$, $V = 0.44$, $U = 1.7$

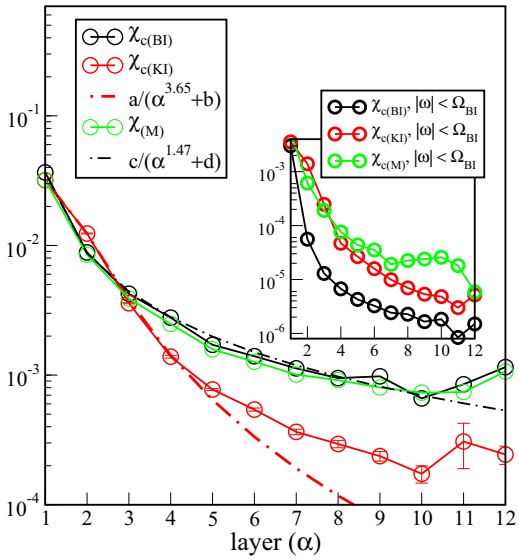

FIG. 8. (Color online) The integrated spectral weight difference [between the disordered and the clean systems, see Eq. (29)] as a function of the layer index for a system of a single doped Kondo insulator interfaced with (a) 11 clean band insulators (black); (b) 11 clean Kondo insulators (red) and (c) 11 metallic layers (green). The main panel is the spectral weight difference with a cutoff, $\lambda \to \infty$. In the inset, $\Omega_{\rm BI} = \frac{1}{2}(-t_{||} + \sqrt{t_{||}^2 + 4V^2})$, representing the hybridization gap edge of an isolated band insulator, has been used as the cutoff (λ) in energy space to get the spectral weight difference at "low" energies ($|\omega| < \Omega_{\rm BI}$). The dot-dashed lines are algebraic decay fits, with black for (a) and (c), and red for (b). $U = 1.7$ in the Kondo insulating layers, $V = 0.44$ in both the band insulating and Kondo insulating layers, the interlayer hopping is set to $t_\perp = 0.5$.

out, as seen in Fig. 8. The spectral weight difference defined in Eq. (29) decreases sharply with distance from the disordered Kondo insulator layer for all the three cases considered (interfacing the disordered Kondo insulator with either 11 metals, or 11 band/Kondo insulators) thus far. These spectral weight changes quantify the proximity effects of disorder, in the absence or presence of interactions. The fits of the spectral weight difference (dot-dashed lines in figure. 8) show that the proximity effects decay algebraically with increasing distance from the boundary layer. Such a decay profile indicates that changes made in the boundary layer can penetrate quite deep into the system.

Apart from the overall decay profile, there are subtle aspects of the spectral weight difference that we highlight now. The main panel in Fig. 8 shows the spectral weight difference computed over all frequency scales ($\lambda \to \infty$). The spectral changes in the noninteracting as well as interacting layers look similar up to the third layer, beyond which the Kondo insulating layers are far less affected than the non-interacting metallic or band-insulating layers. However, the low-frequency spectral weight difference ($\lambda = \Omega_{\rm BI}$), shown in the inset, presents an entirely different picture. The band insulators are seen to be least affected, since the spectral weight difference drops rapidly by over a decade even for the layer adjacent to the disordered Kondo insulator boundary layer. In contrast, the metallic and Kondo-insulating layers experience similar levels of spectral changes due to the disorder in the boundary layer. Thus, when viewed over all scales, interactions indeed screen the proximity effects of disorder. However, in the neighborhood of the Fermi level, the presence of a spectral gap makes the band-insulator immune to the changes in the boundary layer, and the presence or absence of interactions is irrelevant.

IV. DISCUSSION

For the results in the previous section, it is clear that Kondo hole substitution in a single boundary layer does indeed affect neighboring layers to varying degrees on different energy scales. Although we have considered finite systems, a few general remarks may be made for infinite, periodic structures.

A. f-electron superlattices

A superlattice structure comprises a periodic array of unit cells, each of which consist of a finite number of (m) f-e^- and $(n)c$-e^- layers. For example, in Ref. [23], $(m,4)CeIn_3/LaIn_3$ superlattices were grown and m was tuned. The authors surmised that Kondo hole disorder at the Ce/La interface is inevitable. As shown in Fig. 8, the extent of proximity induced disorder effects is appreciable in the neighboring layers. Owing to the periodic nature of a superlattice, it is thus expected that this proximity effect would be even more pronounced stemming from penetration of disorder effects from the adjacent unit cells of the superlattice.

B. A scenario for disorder-induced non-Fermi liquid

Thus far, we have considered the particle-hole symmetric limit. However, an interesting situation might emerge by varying the chemical potential such that the system does not have particle-hole symmetry. Dynamical effects of impurity scattering even at the single-site mean field level have been shown (in Ref. [28]) to lead to a non-Fermi liquid form of the average self-energy. Thus the Kondo hole disordered layers in such an array of f-electron layers would show non-Fermi liquid behavior. The non-Fermi liquid nature of the Kondo hole disordered layers would thus introduce a further anisotropy in the system that would possibly manifest itself in the transport properties of these systems. Moreover, if the Ce/La interfaces in the superlattice unit cell are separated by a larger number of clean layers, the non-Fermi liquid effects would be expected to attenuate. Hence a non-Fermi liquid to Fermi liquid crossover can be expected simply by increasing the ratio of the number of layers to the number of Ce/La interfaces.

C. Anderson localization

One of the important consequences of disorder, ignored in this work, is that of Anderson localization (AL). The CPA employed here to treat disorder effects is incapable of incorporating AL. The addition of coherent back-scattering and deep trap physics beyond CPA should lead to profound consequences for the adjacent layers. A first step in this direction could be the incorporation of the (single site) typical medium theory (TMT) [43] in the context of such layered systems. A subsequent advancement would then be an

systematic inclusion of nonlocal dynamical corrections to the TMT. The typical medium-dynamical cluster approximation (TMDCA) developed recently [44] has been found to be an excellent approach for obtaining the correct phase diagram of the noninteracting Anderson model. It would be interesting to extend the TMDCA for interacting models and explore the interplay of Anderson localization physics and strong interactions in layered systems.

V. SUMMARY AND CONCLUSIONS

In this work, we have employed the inhomogeneous dynamical mean-field theory [19] framework to obtain self-consistent many-body solutions for layered Kondo hole substituted f-electron systems. The substitutional disorder, treated within the coherent potential approximation, was introduced in a single boundary layer, and the consequent spectral changes in the neighboring layers were explored. Three distinct types of clean adjacent layers were considered: (a) noninteracting metals (disordered Kondo insulator/metals), (b) noninteracting band insulators (disordered Kondo insulator/band insulator), and (c) several clean Kondo insulators.

Combining simple analytical expressions for bilayer and trilayer systems with full numerical calculations using the local moment approach, we have (a) explained the strong renormalization of the low-energy spectra of the proximal layers, (b) spectral interference among the layers in presence of an inter-layer coupling ($t_\perp$), and (c) a mechanism for penetration of Kondo hole disorder-induced incoherence into clean layers. We highlight the differences between three distinct types of interfaces with a disordered Kondo insulator layer. We also demonstrate that, in addition to a robust low energy quasiparticle peak [20], proximity effects of interactions also manifest through the appearance of minute Hubbard bands in the neighboring noninteracting layers.

A finite concentration of Kondo holes leads to the formation of an impurity band at the Fermi level in a Kondo insulator [41], thus creating metallic states in the otherwise gapped insulator. In the layered geometry, these disorder-induced metallic states can further tunnel into the immediately neighboring clean Kondo insulator, rendering a quadratic bending in its Kondo hybridization gap edge. This further induces metallic states in the f-e^- spectra of the nearest-neighbor layer. These disorder-induced states do propagate into the further layers but the tunneling is attenuated by the ω^2 factor for each layer and hence is too small to be observed beyond the nearest-neighbor layer. Introduction of disorder further destroys the proximity effect of interactions. We showed that a manifestation of proximity induced interaction effect, on the adjacent noninteracting layers, is the appearance of tiny Hubbard bands and a proximal Kondo effect induced low frequency spectral renormalization. This proximity effect of interactions, on the noninteracting layers, is mitigated when they are coupled to a disordered Kondo insulator layer.

The presence of disorder induces spectral weight transfer from the high-energy Hubbard bands to the low energy Kondo scaling regime not only in the disordered Kondo insulator but in the adjacent clean layers as well. We have quantified the penetration of disorder effects in these interfaces through the spectral weight difference function (29). The spectral weight difference is maximum in the disordered Kondo insulator and decays algebraically with distance from the disordered Kondo insulator layer.

Our analysis implies that, while for thin films, the spectral weight difference of the clean layers is appreciable only until the third neighboring layer; for superlattice geometries, this effect of penetration of disorder would be quite pronounced due to the occurrence of multiple disordered interfaces.

We foresee a Fermi liquid to non-Fermi liquid crossover in the transport properties across disordered interfaces by tuning the number of disordered layers. The full study of such a crossover and inclusion of localization effects beyond the coherent potential approximation will be the subjects of future projects.

ACKNOWLEDGMENTS

This work is supported by NSF DMR-1237565, NSF EPSCoR Cooperative Agreement No. EPS-1003897 with additional support from the Louisiana Board of Regents, and the DOE Computational Materials and Chemical Sciences Network (CMCSN) SC0007091. S.S. acknowledges the support of CSIR, India. S.S. also acknowledges the hospitality of the department of Physics & Astronomy at Louisiana State University.

[1] A. Ohtomo, D. Muller, J. Grazul, and H. Hwang, Artificial charge-modulation in atomic-scale perovskite titanate superlattices, Nature (London) **419**, 378 (2002).

[2] K. Yoshimatsu, T. Okabe, H. Kumigashira, S. Okamoto, S. Aizaki, A. Fujimori, and M. Oshima, Dimensional-crossover-driven metal-insulator transition in $SrVO_3$ ultrathin films, Phys. Rev. Lett. **104**, 147601 (2010).

[3] K. Yoshimatsu, K. Horiba, H. Kumigashira, T. Yoshida, A. Fujimori, and M. Oshima, Metallic quantum well states in artificial structures of strongly correlated oxide, Science **333**, 319 (2011).

[4] S. Okamoto, Anomalous mass enhancement in strongly correlated quantum wells, Phys. Rev. B **84**, 201305 (2011).

[5] M. Potthoff and W. Nolting, Effective mass at the surface of a fermi liquid, Physica B **259**, 760 (1999).

[6] N. Reyren, S. Thiel, A. D. Caviglia, L. F. Kourkoutis, G. Hammerl, C. Richter, C. W. Schneider, T. Kopp, A.-S. Retschi, D. Jaccard, M. Gabay, D. A. Muller, J.-M. Triscone, and J. Mannhart, Superconducting interfaces between insulating oxides, Science **317**, 1196 (2007).

[7] J. A. Bert, B. Kalisky, C. Bell, M. Kim, Y. Hikita, H. Y. Hwang, and K. A. Moler, Direct imaging of the coexistence of ferromagnetism and superconductivity at the $LaAlO_3/SrTiO_3$ interface, Nat. Phys. **7**, 767 (2011).

[8] X. W. Ariando, G. Baskaran, Z. Q. Liu, J. Huijben, J. B. Yi, A. Annadi, A. R. Barman, A. Rusydi, S. Dhar, Y. P. Feng, J. Ding, H. Hilgenkamp, and T. Venkatesan, Electronic phase separation at the $LaAlO_3/SrTiO_3$ interface, Nat. Commun. **2**, 188 (2011).

[9] P. Zubko, S. Gariglio, M. Gabay, P. Ghosez, and J.-M. Triscone, Interface physics in complex oxide heterostructures, Ann. Rev. Condens. Matter Phys. **2**, 141 (2011).

[10] M. Potthoff and W. Nolting, Metallic surface of a Mott insulator–Mott insulating surface of a metal, Phys. Rev. B **60**, 7834 (1999); S. Schwieger, M. Potthoff, and W. Nolting, Correlation and surface effects in vanadium oxides, *ibid.* **67**, 165408 (2003); M. Potthoff and W. Nolting, Dynamical mean-field study of the Mott transition in thin films, Eur. Phys. J. B **8**, 555 (1999); Surface metal-insulator transition in the Hubbard model, Phys. Rev. B **59**, 2549 (1999); The large-U Hubbard model for a semi-infinite crystal: A moment approach and an energy-dependent recursion method, J. Phys.: Condens. Matter **8**, 4937 (1996).

[11] S. Okamoto and A. J. Millis, Spatial inhomogeneity and strong correlation physics: A dynamical mean-field study of a model Mott-insulator–band-insulator heterostructure, Phys. Rev. B **70**, 241104 (2004); Interface phenomena in correlated electron systems, Physica B: Condens. Matter **359-361**, 1378 (2005); Interface ordering and phase competition in a model Mott-insulator–band-insulator heterostructure, Phys. Rev. B **72**, 235108 (2005).

[12] H. Zenia, J. K. Freericks, H. R. Krishnamurthy, and T. Pruschke, Appearance of "fragile" fermi liquids in finite-width Mott insulators sandwiched between metallic leads, Phys. Rev. Lett. **103**, 116402 (2009).

[13] A. Euverte, F. Hébert, S. Chiesa, R. T. Scalettar, and G. G. Batrouni, Kondo screening and magnetism at interfaces, Phys. Rev. Lett. **108**, 246401 (2012).

[14] H. Ishida and A. Liebsch, Embedding approach for dynamical mean-field theory of strongly correlated heterostructures, Phys. Rev. B **79**, 045130 (2009).

[15] H. Ishida and A. Liebsch, Cluster dynamical mean-field study of strongly correlated heterostructures: Correlation-induced reduction of proximity effect, Phys. Rev. B **82**, 045107 (2010).

[16] H. Ishida and A. Liebsch, First-order metal-to-metal phase transition and non-Fermi-liquid behavior in a two-dimensional Mott insulating layer adsorbed on a metal substrate, Phys. Rev. B **85**, 045112 (2012).

[17] R. W. Helmes, T. A. Costi, and A. Rosch, Kondo proximity effect: How does a metal penetrate into a Mott insulator? Phys. Rev. Lett. **101**, 066802 (2008).

[18] A. Rüegg, S. Pilgram, and M. Sigrist, Strongly renormalized quasi-two-dimensional electron gas in a heterostructure with correlation effects, Phys. Rev. B **75**, 195117 (2007); Aspects of metallic low-temperature transport in Mott-insulator/band-insulator superlattices: Optical conductivity and thermoelectricity, **77**, 245118 (2008).

[19] J. K. Freericks, Dynamical mean-field theory for strongly correlated inhomogeneous multilayered nanostructures, Phys. Rev. B **70**, 195342 (2004).

[20] R. Peters, Y. Tada, and N. Kawakami, Kondo effect in f-electron superlattices, Phys. Rev. B **88**, 155134 (2013).

[21] Y. Tada, R. Peters, and M. Oshikawa, Dimensional crossover in layered f-electron superlattices, Phys. Rev. B **88**, 235121 (2013).

[22] S. Okamoto and T. A. Maier, Enhanced superconductivity in superlattices of high-T_c cuprates, Phys. Rev. Lett. **101**, 156401 (2008).

[23] H. Shishido, T. Shibauchi, K. Yasu, T. Kato, H. Kontani, T. Terashima, and Y. Matsuda, Tuning the dimensionality of the heavy fermion compound $CeIn_3$, Science **327**, 980 (2010).

[24] R. Peters and N. Kawakami, Surface density of states of layered f-electron materials, Phys. Rev. B **89**, 041106 (2014).

[25] C. Grenzebach, F. B. Anders, G. Czycholl, and T. Pruschke, Influence of disorder on the transport properties of heavy-fermion systems, Phys. Rev. B **77**, 115125 (2008).

[26] M. Shimozawa, T. Watashige, S. Yasumoto, Y. Mizukami, M. Nakamura, H. Shishido, S. K. Goh, T. Terashima, T. Shibauchi, and Y. Matsuda, Strong suppression of superconductivity by divalent ytterbium Kondo holes in $CeCoIn_5$, Phys. Rev. B **86**, 144526 (2012).

[27] R. K. Kaul and M. Vojta, Strongly inhomogeneous phases and non-Fermi-liquid behavior in randomly depleted Kondo lattices, Phys. Rev. B **75**, 132407 (2007).

[28] N. S. Vidhyadhiraja and P. Kumar, Non-Fermi-liquid behavior from dynamical effects of impurity scattering in correlated Fermi liquids, Phys. Rev. B **88**, 195120 (2013).

[29] E. Feenberg, A note on perturbation theory, Phys. Rev. **74**, 206 (1948); E. N. Economou, *Green's Functions in Quantum Physics* (Springer-Verlag, Berlin, 2006).

[30] D. E. Logan, M. P. Eastwood, and M. A. Tusch, A local moment approach to the Anderson model, J. Phys.: Condens. Matter **10**, 2673 (1998).

[31] M. R. Galpin and D. E. Logan, Single-particle dynamics of the Anderson model: A two-self-energy description within the numerical renormalization group approach, J. Phys.: Condens. Matter **17**, 6959 (2005).

[32] N. S. Vidhyadhiraja, V. E. Smith, D. E. Logan, and H. R. Krishnamurthy, Dynamics and transport properties of Kondo insulators, J. Phys.: Condens. Matter **15**, 4045 (2003).

[33] N. S. Vidhyadhiraja and D. E. Logan, Dynamics and scaling in the periodic Anderson model, Eur. Phys. J. B **39**, 313 (2004).

[34] D. E. Logan and N. S. Vidhyadhiraja, Dynamics and transport properties of heavy fermions: Theory, J. Phys.: Condens. Matter **17**, 2935 (2005).

[35] N. S. Vidhyadhiraja and D. E. Logan, Optical and transport properties of heavy fermions: Theory compared to experiment, J. Phys.: Condens. Matter **17**, 2959 (2005).

[36] M. T. Glossop and D. E. Logan, Local quantum phase transition in the pseudogap Anderson model: Scales, scaling and quantum critical dynamics, J. Phys.: Condens. Matter **15**, 7519 (2003); Spectral scaling and quantum critical behaviour in the pseudogap Anderson model, Europhys. Lett. **61**, 810 (2003); D. E. Logan and M. T. Glossop, A local moment approach to magnetic impurities in gapless Fermi systems, J. Phys.: Condens. Matter **12**, 985 (2000); M. R. Galpin and D. E. Logan, A local moment approach to the gapped Anderson model, Eur. Phys. J. B **62**, 129 (2008).

[37] R. Bulla, M. T. Glossop, D. E. Logan, and T. Pruschke, The soft-gap Anderson model: Comparison of renormalization group and local moment approaches, J. Phys.: Condens. Matter **12**, 4899 (2000).

[38] W.-C. Yueh, Eigenvalues of several tridiagonal matrices, Appl. Math. E-Notes **5**, 66 (2005).

[39] M. Potthoff, Correlated electrons at metal surfaces, Habilitation Thesis, Humboldt-Universität zu Berlin, Berlin, 1999.

[40] P. Aynajian, E. H. da Silva Neto, A. Gyenis, R. E. Baumbach, J. D. Thompson, Z. Fisk, E. D. Bauer, and A. Yazdani, Visualizing heavy fermions emerging in a quantum critical Kondo lattice, Nature (London) **486**, 201 (2012).

[41] P. Schlottmann, Influence of a Kondo-hole impurity band on magnetic instabilities in Kondo insulators, Phys. Rev. B **54**, 12324 (1996); P. S. Riseborough, Collapse of the coherence gap in Kondo semiconductors, *ibid.* **68**, 235213 (2003); T. Mutou, Effects of magnetic-ion dilution in Kondo insulators, *ibid.* **64**, 165103 (2001).

[42] P. Schlottmann, Impurity bands in Kondo insulators, Phys. Rev. B **46**, 998 (1992).

[43] V. Dobrosavljević, A. A. Pastor, and B. K. Nikolić, Typical medium theory of Anderson localization: A local order parameter approach to strong-disorder effects, Europhys. Lett. **62**, 76 (2003).

[44] C. E. Ekuma, H. Terletska, K.-M. Tam, Z.-Y. Meng, J. Moreno, and M. Jarrell, Typical medium dynamical cluster approximation for the study of Anderson localization in three dimensions, Phys. Rev. B **89**, 081107 (2014).